

Ion mobilities in Xe/Ne and other rare-gas mixturesD. Piscitelli,¹ A. V. Phelps,² J. de Urquijo,³ E. Basurto,⁴ and L. C. Pitchford¹¹*Centre de Physique des Plasmas et Applications de Toulouse (CPAT), UMR 5002 CNRS, 118 route de Narbonne, 31062 Toulouse, France*²*JILA, University of Colorado and National Institute of Technology, Boulder, Colorado, USA*³*Centro de Ciencias Físicas, Universidad Nacional Autónoma de México, Post Office Box 48-3, 62251, 80309-0440 Cuernavaca, Moreno, Mexico*⁴*Departamento de Ciencias Básicas, Universidad Autónoma Metropolitana, 02200 México Distrito Federal, Mexico*

(Received 13 May 2003; published 29 October 2003)

The ion mobility or drift velocity data important for modeling glow discharges in rare gas mixtures are not generally available, nor are the ion-neutral scattering cross sections needed to calculate these data. In this paper we propose a set of cross sections for Xe^+ and Ne^+ collisions with Xe and Ne atoms. Ion mobilities at 300 K calculated using this cross section set in a Monte Carlo simulation are reported for reduced field strengths, E/N , up to $1500 \times 10^{-21} \text{ V m}^2$, in pure gases and in Xe/Ne mixtures containing 5% and 20% Xe/Ne, which are mixtures of interest for plasma display panels (PDPs). The calculated Xe^+ mobilities depend strongly on the mixture composition, but the Ne^+ mobility varies only slightly with increasing Xe in the mixture over the range studied here. The mobilities in pure gases compare well with available experimental values, and mobilities in gas mixtures at low E/N compare well with our recent measurements which will be published separately. Results from these calculations of ion mobilities are used to evaluate the predictions of Blanc's law and of the mixture rule proposed by Mason and Hahn [Phys. Rev. A **5**, 438 (1972)] for determining the ion mobilities in mixtures from a knowledge of the mobilities in each of the pure gases. The mixture rule of Mason and Hahn is accurate to better than 10% at high field strengths over a wide range of conditions of interest for modeling PDPs. We conclude that a good estimate of ion mobilities at high E/N in Xe/Ne and other binary rare gas mixtures can be obtained using this mixture rule combined with known values of mobilities in parent gases and with the Langevin form for mobility of rare gas ions ion in other gases. This conclusion is supported by results in Ar/Ne mixtures which are also presented here.

DOI: 10.1103/PhysRevE.68.046408

PACS number(s): 51.10.+y, 51.50.+v, 52.20.Hv

I. INTRODUCTION

This motivation for the work reported here is to improve the data base for modeling glow discharge based devices. The ion mobility or drift velocity data needed for modeling glow discharges in rare gas mixtures are not generally available, nor are the ion-neutral scattering cross sections which could be used to calculate these data. We are particularly interested here with Xe/Ne mixtures where xenon is the minority gas and which are used in plasma display panels (PDPs) [1]. The electrical properties of glow discharges are determined to a large extent by the ion transport through the high field sheath in front of the cathode, and ion mobility data as a function of the reduced field strength, E/N , the ratio of the electric field to the gas density ratio, are needed up to about 1500 Td ($1 \text{ Td} = 10^{-21} \text{ V m}^2$) for PDP modeling, for example. Where data for ion mobilities are not available, Blanc's law [2] or other rough estimates have been used [3]. Because of the large uncertainty in other input data in the models [1], notably in the secondary electron emission coefficients, γ , for ions bombarding the MgO coating on the dielectric surfaces in the case of PDP models, relatively little attention has been paid to the uncertainties in the ion mobility data. In order that uncertainty in the ion mobility data not be the dominant source of uncertainty in calculations of the electrical characteristics of PDPs, we estimate that these mobility data must be accurate to some tens of percent. As shown below, predictions from Blanc's law exceed this tolerance. Thus, while it is not necessary to have very precise

ion mobility data, improvements are needed in the ion mobility data to improve the accuracy of the models.

In this paper we report Monte Carlo calculations of Xe^+ and Ne^+ mobilities in pure gases and in 5% and 20% Xe/Ne mixtures. The Xe^+ and Ne^+ scattering cross sections used in these calculations are also reported here. These Monte Carlo results are used to evaluate ion mobilities determined from Blanc's law and the mixture rule of Mason and Hahn [4], the latter of which is found to yield ion mobilities accurate to within about 10% at high E/N . The Mason and Hahn mixture rule is then used to generate ion mobility data in other Xe/Ne mixtures and in Ar/Ne mixtures. Predictions from the mixture rule are within 10% of the Monte Carlo calculations in all Ar/Ne mixtures for E/N greater than 200 Td. We have chosen to use develop Monte Carlo technique for these studies, but an alternate approach would have been to use the three-temperature theory as discussed, for example, in Ref. [5].

We have measured ion mobilities in Xe/Ne mixtures, and preliminary results were presented by de Urquijo *et al.* [6]. Our more recent experimental results agree very well with calculations at low E/N where the experiments are more reliable. A detailed analysis of the experiments in gas mixtures will be published separately.

This paper is organized as follows. A Monte Carlo simulation is used to calculate the ion mobilities, and this is briefly described in Sec. II. The cross section data are presented in Sec. III, and results from the Monte Carlo calculation of the ion mobilities in Xe/Ne mixtures is shown in Sec. IV. In Sec. V we show comparisons of our Monte Carlo

calculations with predictions from mixture rules for Xe/Ne and for Ar/Ne mixtures. Conclusions are given in Sec. VI.

II. CALCULATION OF ION MOBILITIES

The ion mobilities, or more precisely, the ion drift velocities v_d , are determined from a Monte Carlo simulation of the motion of ions between two infinite, parallel electrodes, separated by a distance d across which a voltage V is applied. The volume between the electrodes is filled with a binary gas mixture, and the number densities of the two neutral species are N_1 and N_2 , respectively. The total gas density is N . Ions of each gas species are considered and they are subjected to the combined influence of a uniform electric field or strength E and collisions with the neutral background gas. We suppose that the neutral background gas temperature is 300 K. The ions undergo collisions with the neutrals, and the angular scattering in the center of mass reference frame is modeled as the sum of isotropic and backward-scattered components (see Sec. III). As has been pointed out by Phelps [7], this way of representing the differential scattering cross section is consistent with measured charge transfer cross sections and previously measured ion mobilities, and it is convenient for use in Monte Carlo simulations.

Our Monte Carlo simulation is standard. Ions are injected at the anode with zero initial velocity and their motion between collisions in a uniform electric field is determined by Newton's equations of motion. The time between collisions is determined using the null collision technique [8]. When a collision takes place, the nature of the collision is determined by comparing a random number to the cumulative sum of the collision frequencies normalized to total (sum of real and null) collision frequency. For each ion species there are four possible results of a collision; null collision, isotropic scattering with the parent gas atom, backscattering with the parent gas atom, or isotropic scattering from the second atom species in the mixture. If the collision is null, the ions continue their trajectories as if nothing had happened. For backscatter collisions, the ion velocity in the laboratory frame after the collision is the same as that of the neutral collision partner before the collision (180° scattering in the center of mass frame). For isotropic collisions, the direction of the ion velocity vector in the center of mass reference frame is randomized. Hagelaar [9] has emphasized that the direction of the center of mass ion velocity after an isotropic collision can be determined simply by selecting random angles from distributions uniform in the azimuthal angle and in the cosine of the polar angle.

The ion drift velocity was determined in two different ways. First, we follow one ion through a very long drift distance, dividing the distance into uniform segments of length dx and calculating the drift velocity through each segment as the ratio of dx to the transit time dt through the segment. The ion drift velocity is then calculated as the average drift velocity through a large number of segments. The product of the gas pressure and the gap spacing, pd , is several torr cm. Second, we simulated the drift tube experiments of Basurto *et al.* [10] releasing a large number of ions (several 1000) from the anode and noting the transit time to the

cathode for each ion. The drift velocity in this latter case is the drift distance divided by the average of the ion transit times. Provided the ion drift velocity is in equilibrium with the electric field, these drift velocities are equal. We return to the question of equilibrium below in Sec. IV.

We report our Monte Carlo results in terms of the reduced ion mobility μN , which is determined from the drift velocity v_d as follows:

$$\mu N = \frac{v_d}{E/N}. \quad (1)$$

We use SI units for the reduced mobility, i.e., $\text{m}^{-1} \text{V}^{-1} \text{s}^{-1}$, and the reduced electric field strength E/N is in units of Td (Townsend) where $1 \text{ Td} = 10^{-21} \text{ V m}^2$.

III. ION-NEUTRAL SCATTERING CROSS SECTIONS

For the purpose of a Monte Carlo calculation, it is convenient to approximate the true, but unknown, differential elastic scattering cross section $I(\varepsilon, \theta)$ of an ion colliding with its parent atom as the sum of an isotropic (in the center-of-mass frame) component $Q_{iso}(\varepsilon)$ and a backward scattered component $Q_b(\varepsilon)$,

$$I(\varepsilon, \theta) \approx Q_{iso}(\varepsilon)/4\pi + Q_b(\varepsilon)\delta(\theta - \pi)/2\pi \sin \theta, \quad (2)$$

where ε is the relative energy, θ is the scattering angle in the center-of-mass reference frame, and δ is the Dirac delta function. The diffusion cross section Q_d in our scattering model [7] is given by $Q_d = Q_{iso} + 2Q_b$. In the absence of inelastic collisions, the momentum transfer cross section Q_m is the same as Q_d . The effect of inelastic collisions on the respective definitions is discussed in Ref. [11].

This form for the differential scattering in Eq. (2) is an approximation, and the differential cross sections proposed in this section are interim recommendations pending the availability of more accurate data [12].

The cross sections used for calculating the mobilities of Xe^+ and Ne^+ are shown in Figs. 1 and 2, respectively. (Note that the range of energies shown in these figures is far larger than needed for calculations of mobilities but may be useful in other contexts.) These are plotted against the ion energy in the laboratory system so as to make more obvious the similarities and differences in cross sections for ions of a given energy moving through the mixture. That is, for the ion energies significantly above thermal which are of greatest interest in this paper, plots of cross sections versus laboratory energy allow one to compare the relative importance of collisions of a given ion with various target atoms without making transformations of energy between laboratory and center-of-mass frames. For use in a Monte Carlo simulation, however, it is convenient to have analytical expressions for the cross sections as functions of relative energy, and these are given below. Recall that the relative energy is equal to the ion energy in the laboratory frame multiplied by the ratio of the target atom mass to the sum of the target atom and the ion masses, if we assume the target atom is at rest. That is, the relative energy of the collision partners is one-half the ion energy in the laboratory frame for ions moving in their

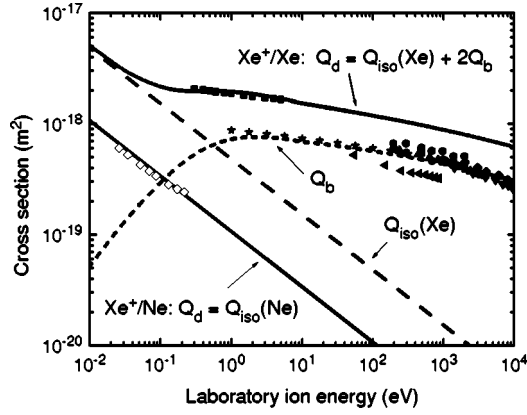


FIG. 1. Cross sections for elastic scattering of Xe^+ with Xe and with Ne versus ion energy in the laboratory reference frame. The short-dashed curve is the backward scattered component and the long-dashed curve is the isotropic component for elastic collisions of Xe^+ with Xe. The upper and lower solid curves are the diffusion cross section for Xe^+ with Xe and Ne, respectively, in this scattering model. The points show experimental data. The symbols and references are as follows: \blacktriangleleft , Ref. [13]; \blacktriangledown , Ref. [14]; \star , Ref. [16]; \blacktriangle , Ref. [14]; \diamond , Ref. [24]; \blacklozenge , Ref. [17]; \blacksquare , Ref. [21]; and \star , Ref. [18].

parent gas. For Xe^+ in Ne, the relative energy is 0.13 times the Xe^+ energy in the laboratory frame and for Ne^+ in Xe, the factor is 0.87.

A. Xe^+ in xenon and neon

The cross sections for elastic scattering of Xe^+ ions with Xe are shown in Fig. 1. The short-dashed curve is the back-

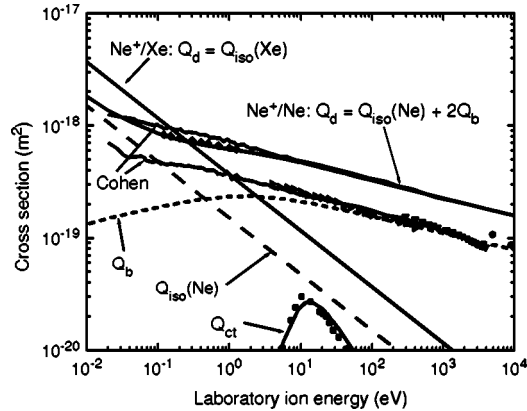


FIG. 2. Cross sections for elastic scattering of Ne^+ with Xe and with Ne versus ion energy in the laboratory reference frame. The isotropic and backscatter components of the Ne^+ /Ne scattering cross section are indicated by the long-dash and the short-dash lines, respectively. The solid lines labeled Ne^+ /Xe and Ne^+ /Ne are the diffusion cross sections for target Xe or Ne atoms as indicated, and the solid curves labeled “Cohen” are from the quantum mechanical calculations of Ref. [28]. Cross sections for asymmetric charge transfer from Ne^+ to Xe^+ are shown in the curve labeled Q_{ct} . The symbols are measured values of charge transfer and diffusion cross sections and references are as follows: \star , Ref. [14]; \blacktriangleright , Ref. [25]; \blacksquare , Ref. [30]; \blacktriangledown , Ref. [15]; and \blacklozenge , Ref. [27].

ward scattered component Q_b and at energies above about 500 eV is obtained by fitting a smooth curve to measured symmetric charge transfer cross sections [13–18]. Such collisions are elastic because there is no change in internal energy of the particles. The long-dashed curve is the isotropic component Q_{iso} for elastic collisions of Xe^+ with Xe. At low energies, the ion scattering is conventionally assumed to be isotropic and equal to the Langevin cross section [19], which can be expressed as

$$Q_{Langevin} = 2\pi a_0^2 (\alpha \text{Ry}/\varepsilon)^{0.5}, \quad (3)$$

where ε is the collision energy, i.e., the relative energy of the colliding particles in the center-of-mass reference frame, α is the polarizability in atomic units of a_0^3 , a_0 is the Bohr radius, and Ry is the Rydberg in the same units as ε . Note that the numerical coefficients in Eq. (3) are consistent with “isotropic scattering” or “spiraling” collisions version of the Langevin cross section [20].

Because of the lack of information regarding the effective isotropic component of Q_d at energies above roughly 0.1 eV, we set it equal to the Langevin cross section at all energies. Next, the backward scattering cross section is adjusted so that the diffusion cross section passes through the cross sections derived from measurements of the mobility of Xe^+ in Xe at laboratory energies from 0.3 to 5 eV [21]. Finally, the backward scattering component at energies below 0.3 eV is adjusted so that the diffusion cross section approaches the isotropic cross section smoothly. Note that according to the model presented here the differential cross section for Xe^+ -Xe scattering becomes isotropic at these low energies and the backward scattering peak used to experimentally determine symmetric charge transfer cross sections at low energies becomes too small to be measured [7].

Analytical expressions for the Xe^+ -Xe cross sections are

$$Q_b = 3.6 \times 10^{-19} [1 + (\varepsilon/0.1)^2]^{0.2} / \varepsilon^{0.42} [1 + (0.09/\varepsilon)^{1.3}] / [1 + (\varepsilon/1000)^{0.25}] \quad (4)$$

and using $\alpha = 27.2$ a.u. [22] in Eq. (3),

$$Q_{iso} = 3.39 \times 10^{-19} / \varepsilon^{0.5}, \quad (5)$$

where ε is the collision energy in eV, i.e., the relative energy of the colliding particles in the center-of-mass reference frame. Note that the backward scattering cross sections given by Eq. (3) for energies above 100 eV are 20% to 30% smaller than the values for charge transfer recommended by Sakabe and Izawa [23].

In the absence of more detailed information, the cross section for elastic scattering of Xe^+ ions with Ne shown in Fig. 1 is taken equal to the Langevin cross section, Eq. (3), at all energies and is assumed to be isotropic ($Q_{iso} = Q_d$). With $\alpha_{Ne} = 2.67$ a.u. [22] in Eq. (3), the analytical expression for the Xe^+ -Ne cross section is

$$Q_{iso} = Q_d = 1.059 \times 10^{-19} / \varepsilon^{0.5}. \quad (6)$$

As shown in Fig. 1, this assumed cross section leads to agreement with diffusion cross sections derived from pub-

lished mobilities for Xe^+ in Ne at energies (in the laboratory frame) from 0.3 to 2 eV [24]. The fact that the diffusion cross section for Xe^+ in Ne is much smaller than that for Xe^+ in Xe at energies interest for mobility calculations, i.e., 0.01 to 10 eV, leads to a strong dependence of the Xe^+ mobility on the mixture composition for low concentrations of xenon, as will be seen below.

B. Ne^+ in neon and xenon

Cross sections for elastic scattering of Ne^+ ions with Ne and Xe are shown in Fig. 2. For elastic collisions of Ne^+ with Ne, the short-dashed curve is the backward scattered component and the long-dashed curve is the isotropic component. The solid curve labeled Ne^+/Ne is the diffusion cross section for Ne^+ with Ne in this scattering model. These curves were obtained by fitting the experimental charge transfer cross section [13,15–17,25,26] and mobility-based diffusion cross section data [27] using the procedure discussed above for Xe^+/Xe collisions. The curves labeled “Cohen” are theoretical results from Cohen and Schneider’s quantum mechanical calculation of the diffusion and charge-transfer cross sections [28]. It will be noted that our Q_b curve drops below the theoretical and experimental charge transfer cross sections at energies near 10 eV because the cross sections represent different aspects of the collision. Our cross sections for collisions of Ne^+ with Ne have the same general behavior as those of Jovanovic *et al.* [29], but differ significantly in detail.

Analytical expressions for the Ne^+/Ne cross sections as a function of relative energy are

$$Q_b = 2.8 \times 10^{-19} / \varepsilon^{0.15} / (1 + 0.8/\varepsilon)^{0.3} \quad (7)$$

and from Eq. (3) with $\alpha = 2.67$ a.u. [22],

$$Q_{iso} = 1.059 \times 10^{-19} / \varepsilon^{0.5}. \quad (8)$$

Because of our use of center-of-mass energies, Q_{iso} is the same as for Xe^+/Xe collisions. Again, the charge transfer cross sections given by Eq. (7) for energies above 100 eV are 20% to 30% smaller than the values recommended by Sakabe and Izawa [23].

The cross section for elastic scattering of Ne^+ with Xe is analogous to what we use for Xe^+ scattering with Ne. That is, the cross section for elastic scattering of Ne^+ with Xe shown by the solid curve in Fig. 2 is taken equal to the Langevin cross section at all energies and is assumed to be isotropic ($Q_{iso} = Q_d$). The fact that the diffusion cross section for Ne^+ in Xe is approximately the same as that for Ne^+ in Ne at ion energies of interest for mobility calculations, e.g., at laboratory energies near 0.3 eV, is manifested in the results below as a relative insensitivity of the Ne^+ mobility to the mixture composition.

An analytical expression for the Ne^+/Xe cross section as a function of relative energy is

$$Q_{iso} = Q_d = 3.39 \times 10^{-19} / \varepsilon^{0.5}. \quad (9)$$

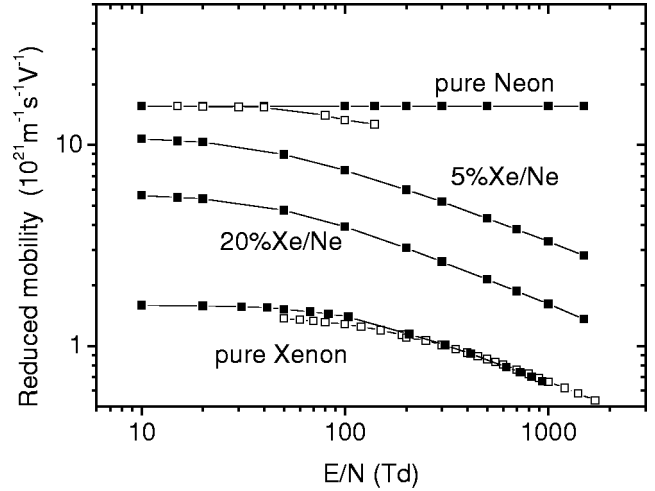


FIG. 3. Calculated (solid symbols) mobility of Xe^+ vs E/N in pure neon, in pure xenon, and in 5% and 20% Xe/Ne mixtures compared to experimental results (open symbols) of Larsen and Elford [21] in pure xenon and of Johnsen and Biondi [24] in pure neon.

For completeness we also show in Fig. 2 the measured cross section for the transfer of charge from Ne^+ to Xe [30,31]. Upper limits to this cross section of $1 \times 10^{-21} \text{ m}^2$ at an average energy of 0.026 eV have been obtained from flowing afterglow experiments [32], while swarm experiments yield an upper limit of $2 \times 10^{-23} \text{ m}^2$ at average laboratory energies from 0.04 to 0.1 eV [33]. A fit to this data shown by the solid curve is

$$Q_{ct} = 5 \times 10^{-21} (\varepsilon - 2.5) / [1 + (\varepsilon/10)^4]^{0.5}. \quad (10)$$

The measured maximum cross section for Xe^{++} formation (not shown) is about an order of magnitude smaller and peaks at 40 eV [30].

Charge transfer from Ne^+ to Xe^+ or Xe^{++} is neglected in our Monte Carlo calculations of the ion mobilities because numerical tests show that it is not important for the conditions reported here.

IV. CALCULATED ION MOBILITIES IN Xe/Ne MIXTURES

In this section we present results of Xe^+ mobilities in pure Xe and Ne and in 5% and 20% Xe/Ne mixtures. We also present calculated Ne^+ mobilities in pure Ne and in the 20% Xe/Ne mixtures. These gas mixtures were chosen because of their relevance to PDPs.

A. Xe^+ mobility in Xe/Ne mixtures

In Fig. 3 we show the Xe^+ mobilities calculated in pure xenon, in pure neon, and in 5% and 20% Xe/Ne mixtures. For comparison, the experimental points (open symbols in the figure) from Larsen and Elford [21] for Xe^+ in pure xenon at 294 K and for Xe^+ in pure neon from Johnsen and Biondi [24] at 300 K are also shown in the figure. In pure

xenon, there is very good agreement over the full range of E/N between our calculations and the measurements of Larsen and Elford.

The Xe^+ mobility is very sensitive to the concentration of Xe in the mixture, especially for small concentrations of Xe and for the higher values of E/N . This sensitivity is due mainly to the large diffusion cross section for Xe^+ scattering with Xe as compared to that with Ne. The cross section ratio from Fig. 1 is 7:1 at 0.1 eV and 16:1 at 1 eV. The only experimental data available in the mixtures was reported in a preliminary form by de Urquijo *et al.* [6]. Comparisons with our more recent experimental results range from good to very good at low E/N and fair for E/N greater than 200 Td. These results will be published separately along with a detailed description of the two systems used for these measurements, the analytical procedures, and a discussion as to the agreement and differences between the present calculations and the measurements.

The experimental data for Xe^+ mobility in pure neon are limited to E/N less than 140 Td. Calculations compare well with experimental results at low E/N . The agreement is acceptable up to 140 Td, but the trend in the experiments is for the mobility to decrease somewhat with E/N . Because the collision frequency ν , used in the calculations for Xe^+ collisions with neon is independent of energy [see Eq. (6)], the calculated mobility is independent of E/N . An exact analytical expression for the mobility can be obtained from momentum transfer theory [22],

$$\mu N = \frac{e}{M_R} \left(\frac{\nu}{N} \right)^{-1}. \quad (11)$$

This can also be written as [34],

$$\mu N = 35.9 \times 10^{-4} \times (6.95/2\pi) \times 2.69 \times 10^{25} / (\alpha M_r)^{0.5} \text{ m}^{-1} \text{ V}^{-1} \text{ s}^{-1}, \quad (12)$$

where the reduced mass M_r is in units of the proton mass and the atomic polarizability in atomic units. Note that the factor $(6.95/2\pi)$ multiplies the conventional expression for the ion mobility in order to take into account our use of the spiraling version of the polarization cross section rather than the ‘‘rigid core’’ version used in conventional mobility formulas. See Table 5-5-1 of Ref. [22] and Sec. IIID of Ref. [35]. The numerical value from Eq. (12) is $1.56 \times 10^{22} \text{ m}^{-1} \text{ V}^{-1} \text{ s}^{-1}$ for Xe^+ in pure neon.

The increasing difference between calculated and measured mobility with increasing E/N suggests in pure neon that the diffusion cross section for Xe^+ collisions with Ne should be modified for high ion energies. However, the available mobility data are not sufficient to propose a better cross section for Xe^+ collisions with Ne at this point.

We have confirmed that anisotropy in the scattering cross sections has no effect on the calculated ion mobility provided the momentum transfer cross section is constant. This result is anticipated from momentum transfer theory, which shows that the ion mobilities depend only on the momentum transfer cross section and not on the assumed angular distribution [22]. This result is also consistent with the conclusions of

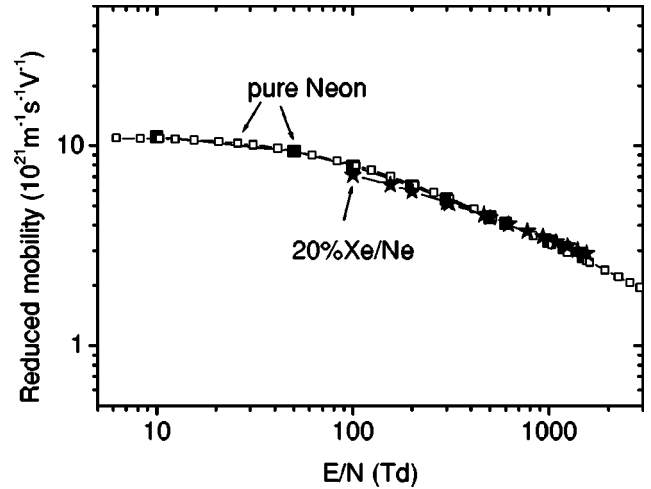


FIG. 4. Calculated mobility of Ne^+ vs E/N in pure neon (■) and 20% Xe/Ne mixtures (★) compared to experimental results (□) of Hegerberg *et al.* [36] for Ne^+ mobilities in pure Ne at 293 K.

Jovanović *et al.* [29] who conclude that anisotropic scattering has little effect on the calculated mobility (but a large effect on the perpendicular diffusion coefficient).

B. Ne^+ mobility in pure neon and in Xe/Ne mixtures

The calculated Ne^+ mobilities in pure neon and in the 20% Xe/Ne mixture are shown in Fig. 4. For comparison, Ne^+ mobilities in pure neon at 293 K measured by Hegerberg *et al.* [36] are shown as open symbols, and the calculated values of the mobility are in excellent agreement with these experimental results and with the recent measurement of Basurto *et al.* [10] (not shown in the figure). As was anticipated above on the basis of the cross sections used in the calculations, the Ne^+ mobilities are not very sensitive to the mixture composition for xenon concentrations up to 20%. The calculated Ne^+ mobilities in the 5% Xe/Ne mixture are almost indistinguishable from the results in pure neon and are therefore not shown in the figure. In the 20% Xe/Ne mixture, the Ne^+ mobility is slightly less than that in pure neon at low E/N and very slightly higher at high E/N . The low E/N decrease is due to fact that the momentum transfer between Ne^+ and Xe at low ion energy more than compensates for the reduced number of Ne^+ with Ne. At higher ion energies, momentum transfer between Ne^+ and Xe no longer compensates for the reduced number of Ne^+ collisions with Ne because the Ne^+ /Xe diffusion cross section decreases with ion energy.

C. Mean ion energies

The range of Xe^+ energies relevant to the calculation of the ion mobilities reported here varies considerably with gas mixture. In Fig. 5 we show the calculated mean energy (in the laboratory frame) of Xe^+ in pure xenon and in the 5% and 20% mixtures vs E/N . A small increase in the percentage of Xe in the mixture leads to a significant change in the mean energy of Xe^+ , as well as in the mobility as seen above. For comparison the mean energies of Ne^+ in pure

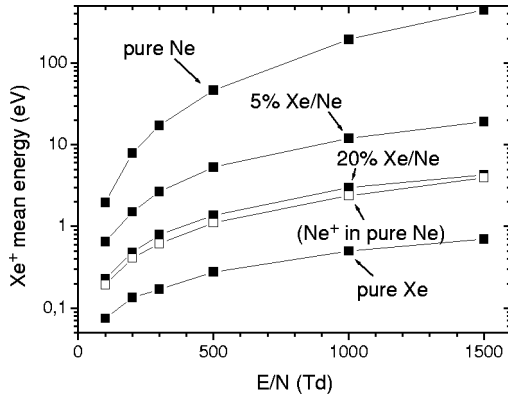


FIG. 5. Calculated Xe^+ mean energy (laboratory frame) vs E/N in pure Xe, pure Ne, and in the 5% and 20% Xe/Ne mixtures. The open symbols are the mean energies calculated for Ne^+ in pure neon.

neon are also shown in the figure. The presence of 5% or 20% Xe in a Xe/Ne mixture has relatively little effect on the mean energy of the Ne^+ . That is, at 1000 Td the mean energy of Ne^+ in 20% Xe/Ne is only 17% higher than that in the pure neon. Recall that the gas temperature in our calculations is 300 K, and this finite gas temperature has an influence on the ion mean energy only for the lowest mean energies (low E/N , pure xenon)

The calculations show that the ion energy distribution functions over the range of conditions in Fig. 5 are almost Maxwellian, and hence the mean energies in Fig. 5 provide information on the range of energies of the cross sections entering into the mobility calculations. The good comparison between calculated and experimental mobilities for the ions in their parent gases provides a measure of confidence of the cross sections up to about 1 eV for Xe^+ and up to about 4 eV for Ne^+ (energies in the laboratory frame).

D. Use of the local field approximation

When the energy gained by the ions in the electric field is locally balanced by energy lost in collisions, the “local field” approximation is said to apply, ions are in “equilibrium with the field,” and the ion mobilities in a given gas mixture are functions of only E/N as we have assumed above. In this section we address the question of when this approximation is valid in Xe/Ne mixtures. According to momentum transfer theory, the exponential time constant, τ_{eq} , describing the approach of the ion drift velocity (or ion mobility) to its equilibrium value, is [37]

$$(\tau_{eq})^{-1} = v'_m = \sum N_i \left(\frac{M_i}{m + M_i} \right) Q_{m,i}(\epsilon_{rel}) v_{rel,i}, \quad (13)$$

where M_i is the mass of the neutral background gas atom, m is the ion mass, and the sum is over all components in the mixture. N_i is the density of the i th component of the mixture. The mass ratio factor comes about by considering the change in laboratory frame velocity of the ion as a result of a collision. That is, momentum exchange between heavy ions and low mass atoms is not efficient and a long time is re-

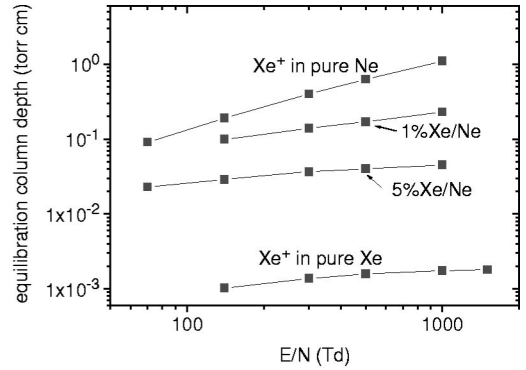


FIG. 6. Equilibration column depth (in units of pressure \times distance) for Xe^+ mobility in pure Xe, pure Ne, and in Xe/Ne mixtures with 1% and 5% Xe.

quired for the heavy ion energy distribution to be in equilibrium with the local reduced field. Thus, the local field approximation is more questionable for Xe^+ mobilities in pure neon and in Xe/Ne mixtures with low concentrations of Xe.

To evaluate the equilibration distance of Xe^+ mobility for different conditions, we simulated drift tube experiments with variable column depth (product of gas pressure and drift distance). The ions are introduced into the drift tube with zero initial velocity, and the details of the evolution, but not the equilibration distance, depend on the initial conditions. The results of these calculations are summarized in Fig. 6 where the equilibration distance is shown as a function of E/N for pure neon, and in 1%, 5%, and 10% Xe/Ne mixtures. The equilibration distance was defined in the calculations as the distance at which the ion mobility has reached within $1/e$ of its final equilibrium (large pd) value. The most evident trend is that the equilibration distance decreases rapidly with increasing Xe concentration, mainly because of the increasing collision frequency but also because momentum transfer is more efficient between particles of equal mass. A slightly longer equilibration distance is required for higher E/N because the ion energies are higher and cross sections lower. The experiments of Johnsen and Biondi [24] for Xe^+ mobility in pure neon were carried out with a minimum pd (product of pressure and distance) of 4.49 torr cm which should assure equilibrium conditions.

In a glow discharge, the electric field is high at the cathode and decreases more or less linearly in the cathode fall. In an abnormal dc glow discharge, the cathode fall thickness depends on gas composition and composition of the surface, but can be 0.1 torr cm (or less at high current density). Use of a local field mobility for ion transport in its parent gas is generally suitable, but it is questionable for minority gas ions when the minority gas is present in small concentrations. The cathode fall thickness in a plasma display panel cell is larger than in a dc glow discharge because the voltage drops before the sheath is fully formed. The sheath length in PDPs in a matrix geometry [1] at the time of the peak current is about 0.8 torr cm for the typical conditions [3], and E/N at the cathode is 1000 to 1500 Td. We estimate that the local field mobility provides an adequate representation of the Xe^+

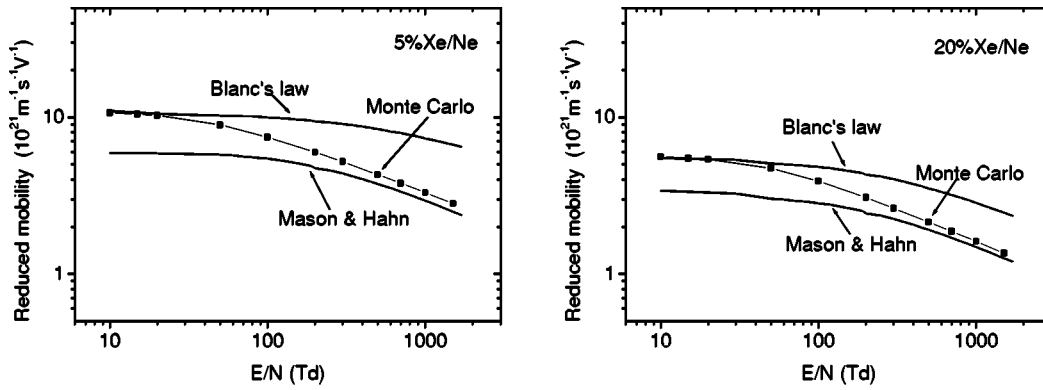


FIG. 7. Xe^+ mobilities vs E/N in 5% and 20% Xe/Ne mixtures predicted from Blanc's law and using the mixture rule of Mason and Hahn. Shown for comparison are Monte Carlo calculations of the Xe^+ mobilities.

transport in the sheath in PDPs in 10% Xe/Ne mixtures, but should be used with caution for xenon concentrations less than 5%.

V. MIXTURE RULES

Different mixture rules have been proposed to calculate transport coefficients of ions in gas mixtures from a knowledge of the transport coefficients in each of the single pure components [2,4,37–39]. The best known of these is Blanc's law which states that the reciprocal of the ion mobility is a linear function of the fractional concentration of either constituent of the mixture. This is generally valid for very low fields (thermal energies) or for the limiting case of constant collision frequency for both gases at all energies. Some mixture rules have been reviewed by Himoudi [40]. A systematic evaluation of the different proposed mixture rules is outside the scope of this paper, although it would be quite useful. Since we are mainly interested in high E/N , we focus here on the mixture rule of Mason and Hahn [4] which was derived from momentum transfer theory for constant cross section and for fields high enough that thermal energy of the neutral collision partner can be neglected. (See also Whealton *et al.* [38] for clarifications on the approximations used in the derivation of this mixture rule.) This mixture rule can be written as

$$\frac{1}{(\mu N)_{mix}^2} = \sum_i \frac{x_i}{(\mu N)_i^2} \left(\frac{m + \bar{M}_{mix}}{m + M_i} \right)^{1/2}, \quad (14)$$

where \bar{M}_{mix} is the weighted, average mass of the mixture expressed as

$$\bar{M}_{mix} = \frac{\sum_i \omega_i M_i}{\sum_i \omega_i} \quad \text{with} \quad \omega_i = \frac{x_i}{(\mu N)_i} \left(\frac{m}{m + M_i} \right)^{3/2}.$$

This mixture rule relates the inverse of the square of the ion mobility in a gas mixture to a weighted average of the inverse squares of the ion mobilities in each of the pure gases.

Results of predictions of Blanc's law and the mixture rule of Mason and Hahn are compared to Monte Carlo calculations of Xe^+ mobilities in 5% and 20% Xe/Ne mixtures in Fig. 7. Not surprisingly, deviations from Blanc's law increase

with increasing field and are as high as 50% at 1000 Td in the 5% mixture. A much better prediction of the ion mobility can be found from the mixture rule of Mason and Hahn, which yields results in good agreement with the Monte Carlo results for Xe^+ mobilities in 5% and 20% Xe/Ne mixtures for E/N greater than 200 Td.

We tested, although not systematically, the mixture rule of Milloy and Robson [37] in the form given by Whealton *et al.* [38] and in the form discussed by Iinuma *et al.* [39]. In the former and for the cases tested, the differences between the Xe^+ ion mobilities predicted using these mixture rules and our calculated values increase with increasing E/N above about 100 Td. Our preliminary calculations suggest a more accurate result can be obtained using the form discussed by Iinuma *et al.* The interpretation of these results is outside the scope of this paper, and our empirical conclusion is that the mixture rule of Mason and Hahn is to be preferred for ion mobilities in gas mixtures at high E/N (> 100 Td) and when symmetric charge transfer can occur.

A difficulty in using mixture rules is that data for ion drift velocities in each of the pure gases is needed. For example, while data for Xe^+ in Xe are available over a wide range of values of E/N , the experimental data for Xe^+ drifting in pure neon is limited to E/N less than 140 Td. Therefore, it is necessary to rely on theory for data at higher E/N using Eqs. (12), for example. From the measured values of Xe^+ drift velocities in pure xenon and the analytical form for the drift velocity of Xe^+ in pure neon, it is possible to deduce Xe^+ drift velocities in Xe/Ne mixtures with a precision sufficient for use in models of plasma display panels.

A. Ion mobilities in other Xe/Ne mixtures

In Fig. 8 we show Xe^+ and Ne^+ mobilities vs E/N in Xe/Ne mixtures containing 3% to 50% Xe calculated using the mixture rule of Mason and Hahn. These are our recommended data for use in PDP models.

B. Ion mobilities in Ar/Ne mixtures

Ion mobilities in other rare gas mixtures are also of technical interest. For example, models of cold-cathode fluorescent lamps of the type used in display lighting require ion

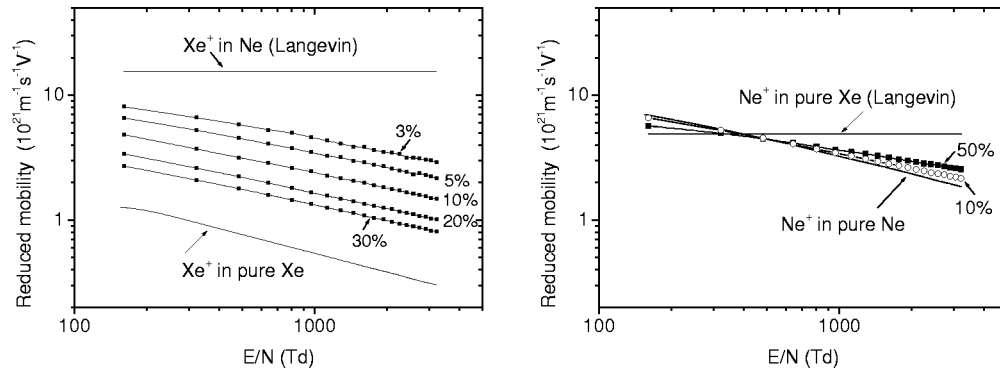


FIG. 8. Reduced mobilities vs E/N in different Xe/Ne mixtures (% Xe in the mixture is indicated) for Xe^+ (left panel) and for Ne^+ (right panel).

mobility data at high fields [41,42]. Ternary mixtures (Xe/Ar/Ne) are used in flat, mercury-free fluorescent lamps for backlighting applications [43]. Also, rare gas mixtures other than Xe/Ne have been studied for the PDP application [1]. We propose that the ion mobility data for E/N greater than about 100 Td needed for modeling gas discharges in binary rare gas mixtures can be deduced with adequate precision using the Mason and Hahn mixture rule, data from the literature for ion mobilities in their parent gases, and from Eq. (12) above for ion mobilities in other rare gases.

To test this hypothesis, we calculated ion mobilities in Ar/Ne mixtures using the Monte Carlo simulation, from Blanc's law and from the mixture rule of Mason and Hahn. The ion mobilities in Ar/Ne mixtures calculated with the Monte Carlo simulation are shown in Fig. 9. The cross sections used in the Monte Carlo simulation for Ar^+ scattering with Ar are from Phelps [7]. The mobility of Ar^+ in pure argon calculated with these cross sections compares very well with available experimental data [44]. The Langevin cross sections [Eq. (3)] are used for Ar^+ scattering with Ne and for Ne^+ scattering with Ar (with a polarizability of 11.11 a.u. for argon atoms [22]). Thus, from Eq. (12), we find a reduced mobility of $1.76 \times 10^{22} \text{ m}^{-1} \text{ V}^{-1} \text{ s}^{-1}$ for Ar^+ in pure Ne and $0.875 \times 10^{22} \text{ m}^{-1} \text{ V}^{-1} \text{ s}^{-1}$ for Ne^+ in pure Ar.

As shown above for Xe^+ mobilities in Xe/Ne mixtures, application of the Mason and Hahn mixture rule to ion mobilities in Ar/Ne mixtures yields mobilities which compare very well with the Monte Carlo results. The relative differ-

ence between the predictions of the Mason and Hahn's mixture rules and Blanc's law are shown in Fig. 10 for Ar^+ and Ne^+ mobilities in different Ar/Ne mixtures as indicated. The fractional differences using the Mason and Hahn mixture rule are somewhat less than those shown in the example of Xe/Ne mixtures above.

VI. CONCLUSIONS

A set of ion-neutral scattering cross sections has been derived and used in a Monte Carlo simulation to calculate the mobilities of Xe^+ and Ne^+ in Xe/Ne gas mixtures. Good agreement is found in the comparisons of calculated and measured mobilities for Xe^+ in pure xenon and for Ne^+ in pure neon. Acceptable agreement is also found for Xe^+ mobilities in pure neon, although there appears to be a systematic increase in the difference with E/N . This acceptable to good agreement shows the usefulness of the cross sections presented here for calculations over the range of energies relevant to our conditions ($< 1 \text{ eV}$ for Xe^+ in xenon and up to about 4 eV for Ne^+ in Ne). We have shown that the distance required for the Xe^+ mobility to be in equilibrium with the local value of E/N is dependent mainly on the gas mixture. While the local field approximation is valid for mixtures with high xenon concentration, it is questionable for PDP conditions for mixtures containing small concentrations (several percent or less) of xenon.

The impetus for this work was the need for ion mobility

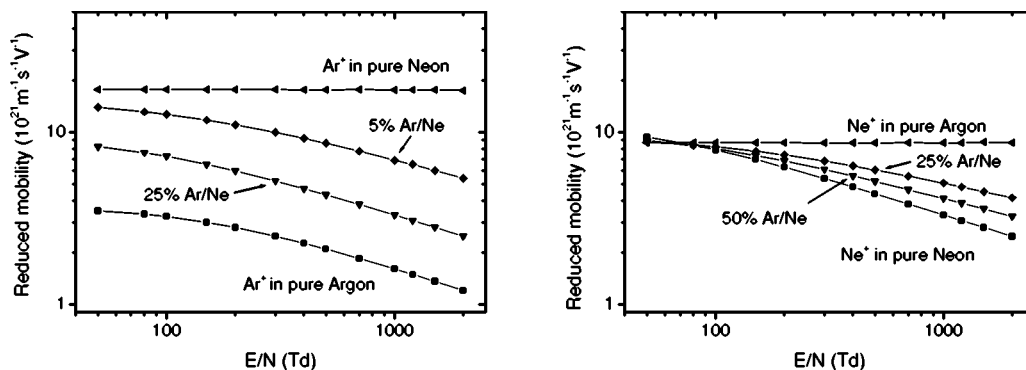


FIG. 9. Calculated reduced mobilities of Ar^+ (left panel) and Ne^+ (right panel) in Ar/Ne mixtures as indicated on the figures.

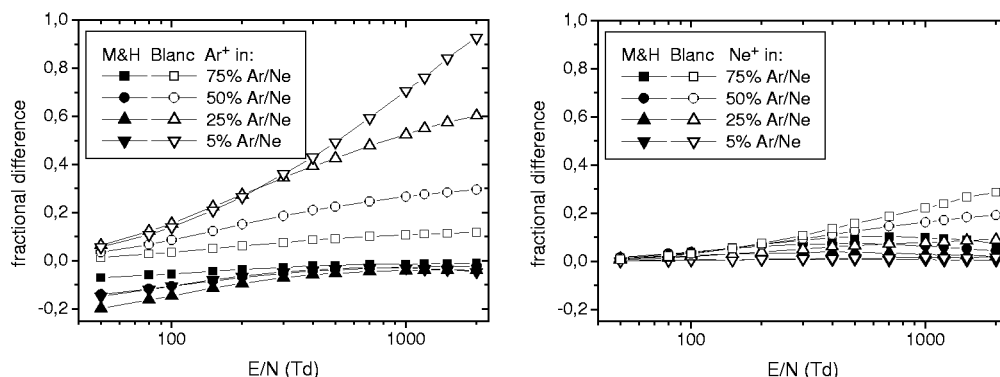


FIG. 10. Fractional difference between Ar^+ (left panel) and Ne^+ (right panel) mobilities predicted by the mixture rules of Blanc and Mason and Hahn (M&H) for the Ar/Ne mixtures as indicated in the legends.

data in Xe/Ne mixtures for models of plasma display panels, PDPs. In the PDP application, the xenon concentrations vary from 3% to 20% Xe in Ne, and ion mobility are needed up to about 1500 Td. The results presented here provide a way of checking the predictions of mixture rules, and we have shown above that acceptably accurate values of the Xe^+ mobilities in arbitrary mixtures of Xe/Ne and for E/N greater than about 100 Td can be very simply obtained using the mixture rule proposed by Mason and Hahn. In order to use this mixture rule, ion mobility data in pure gases are needed. These data are readily available only for ions in their parent rare gas. Lacking data for ion mobilities in rare gases other than their parent, these mobilities can be estimated using the

form derived from a Langevin cross section and given in Eq. (12).

Our recent experimental values of ion mobilities in Xe/Ne mixtures agree well with the calculations at low E/N where the experiments are most accurate. These will be published separately.

ACKNOWLEDGMENTS

D.P. and L.C.P. would like to acknowledge partial support of this work through the French Ministry of Research. Many useful discussions with J.P. Boeuf and G. Hagelaar are also gratefully acknowledged. A.V.P. thanks L.A. Viehland for helpful correspondence.

- [1] J.-P. Boeuf, *J. Phys. D: Appl. Phys.* **36**, R1 (2003).
 [2] A. Blanc, *J. Phys. (Paris)* **7**, 825 (1908).
 [3] J. Meunier, P. Belenguer, and J.-P. Boeuf, *J. Appl. Phys.* **78**, 731 (1995).
 [4] E. A. Mason and H.-S. Hahn, *Phys. Rev. A* **5**, 438 (1972).
 [5] E. A. Mason and A. W. McDaniel, *Transport Properties of Ions in Gases* (Wiley, New York, 1988).
 [6] J. de Urquijo, E. Basurto, A. V. Phelps, D. Piscitelli, and L. C. Pitchford, *Bull. Am. Phys. Soc.* **45**, 47 (2000).
 [7] A. V. Phelps, *J. Appl. Phys.* **76**, 747 (1994).
 [8] H. R. Skullerud, *J. Phys. D: Appl. Phys.* **1**, 1567 (1968).
 [9] G. Hagelaar, Ph.D. thesis, Technical University of Eindhoven, 2000.
 [10] E. Basurto *et al.*, *Phys. Rev. E* **61**, 3053 (2000).
 [11] A. V. Phelps and L. C. Pitchford, *Phys. Rev. A* **31**, 2932 (1985).
 [12] These differential cross sections are interim recommendations pending the availability of more accurate data. An example of large deviations from isotropic scattering at low energies is calculations for Na^+ collisions with Xe [A. V. Phelps, *Proceedings of the XXII International Conference on Photonic, Electronic, and Atomic Collisions*, edited by S. Datz *et al.* (Rinton, Princeton 2001), p. 532].
 [13] J. A. Dillon *et al.*, *J. Chem. Phys.* **23**, 776 (1955).
 [14] I. P. Flaks and E. S. Solov'ev, *Zh. Tekh. Fiz.* **28**, 599 (1958) [*Sov. Phys. Tech. Phys.* **3**, 564 (1958)].
 [15] B. I. Kikiani *et al.*, *Zh. Tekh. Fiz.* **45**, 586 (1975) [*Sov. Phys. Tech. Phys.* **20**, 364 (1975)].
 [16] N. Hishinuma, *J. Phys. Soc. Jpn.* **32**, 1452 (1972).
 [17] R. F. King and C. J. Latimer, *J. Phys. B* **16**, 583 (1983).
 [18] J. S. Miller *et al.*, *J. Appl. Phys.* **91**, 984 (2002).
 [19] E. W. McDaniel, J. B. A. Mitchell, and E. Rudd, *Atomic Collisions: Heavy Particle Projectiles* (Wiley, New York, 1993), pp. 231 and 498.
 [20] From Table 5-5-1 of McDaniel and Mason (see Ref. [22]) it can be seen that there is not a unique cross section for "polarization" scattering. The spiraling cross section we use corresponds to the last entry in this table and differs by a factor of $6.95/2\pi$ from that calculated from a potential given by the polarization interaction at large radii and a "thin rigid core" at small radii. This terminology is that of the second entry in the table.
 [21] P. H. Larsen and M. T. Elford, *J. Phys. B* **19**, 449 (1986).
 [22] E. W. McDaniel and E. A. Mason, *The Mobility and Diffusion of Ions in Gases* (Wiley, New York, 1973), p. 344.
 [23] S. Sakabe and Y. Izawa, *Phys. Rev. A* **45**, 2086 (1992).
 [24] R. Johnsen and M. A. Biondi, *Phys. Rev. A* **20**, 221 (1979).
 [25] W. H. Cramer, *J. Chem. Phys.* **28**, 688 (1958).
 [26] I. P. Flaks, *Zh. Tekh. Fiz.* **31**, 36 (1961) [*Sov. Phys. Tech. Phys.* **6**, 263 (1961)].
 [27] R. Hergerberg, M. T. Elford, and H. R. Skullerud, *J. Phys. B* **15**, 797 (1982).

- [28] J. S. Cohen and B. Schneider, *Phys. Rev. A* **11**, 884 (1975).
- [29] J. V. Jovanović, S. B. Vrhovac, and Z. L. Petrović, *Eur. Phys. J. D* **21**, 335 (2002).
- [30] W. B. Maier II, *Phys. Rev. A* **5**, 1256 (1972).
- [31] W. B. Maier II, *J. Chem. Phys.* **69**, 3077 (1978).
- [32] R. S. Hemsworth *et al.*, *Chem. Phys. Lett.* **5**, 237 (1970).
- [33] R. Johnsen, J. MacDonald, and M. A. Biondi, *J. Chem. Phys.* **68**, 2991 (1978).
- [34] G. Wannier, *Bell Syst. Tech. J.* **32**, 170 (1953).
- [35] G. Heiche and E. A. Mason, *J. Chem. Phys.* **53**, 4687 (1970).
- [36] R. Hegerberg, M. T. Elford, and H. R. Skullerud, *J. Phys. B* **15**, 797 (1982).
- [37] H. B. Milloy and R. E. Robson, *J. Phys. B* **6**, 1139 (1973).
- [38] J. H. Whealton, E. A. Mason, and R. E. Robson, *Phys. Rev. A* **9**, 1017 (1974).
- [39] K. Iinuma, E. A. Mason, and L. A. Viehland, *Mol. Phys.* **61**, 1131 (1987).
- [40] A. Himoudi, Ph.D. thesis, Université Paul Sabatier, Toulouse, 1993.
- [41] H. Sarroukh *et al.*, in *Proceedings of the International Symposium on Plasma Chemistry*, Orléans, France, 2001.
- [42] H. Capdeville, C. Pédoussat, and L. C. Pitchford, *J. Appl. Phys.* **91**, 1026 (2002).
- [43] T. Shiga *et al.*, *J. Light Visual Environ.* **25**, 10 (2001).
- [44] H. W. Ellis *et al.*, *At. Data Nucl. Data Tables* **17**, 177 (1976).